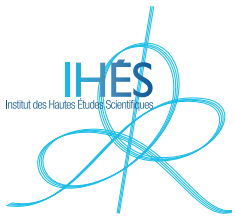

Séminaire Laurent Schwartz

EDP et applications

Année 2016-2017

Josselin Garnier

High-order statistics for the random paraxial wave equation

Séminaire Laurent Schwartz — EDP et applications (2016-2017), Exposé n° IX, 14 p.

<http://slsedp.cedram.org/item?id=SLSEDP_2016-2017____A9_0>

Institut des hautes études scientifiques
Le Bois-Marie • Route de Chartres
F-91440 BURES-SUR-YVETTE
http://www.ihes.fr/

Centre de mathématiques Laurent Schwartz
CMLS, École polytechnique, CNRS, Université Paris-Saclay
F-91128 PALAISEAU CEDEX
http://www.math.polytechnique.fr/

cedram

Exposé mis en ligne dans le cadre du
Centre de diffusion des revues académiques de mathématiques
http://www.cedram.org/

Séminaire Laurent-Schwartz — EDP et applications
Centre de mathématiques Laurent Schwartz, 2016-2017
Exposé n° IX, 1-14

High-order statistics for the random paraxial wave equation

Josselin Garnier*

Abstract

We consider wave propagation in random media in the paraxial regime. We show how to solve the equations for the second- and fourth-order moment of the field in the regime where the correlation length of the medium is smaller than the initial beam width. We quantify the scintillation of the transmitted field and the statistical stability of the Wigner transform. We finally discuss a few applications to correlation-based communication and imaging methods.

1 Wave propagation in random media

In this section we briefly describe how to derive the mathematically tractable Itô-Schrödinger model from the wave equation in a random medium. We consider the three-dimensional scalar wave equation:

$$\frac{1}{c^2(\boldsymbol{x})}\frac{\partial^2 u}{\partial t^2}(t,\boldsymbol{x}) - \Delta_{\vec{\boldsymbol{x}}} u(t,\boldsymbol{x}) = F(t,\boldsymbol{x}). \tag{1}$$

Here the source emits a time-harmonic signal and it is localized in the plane $z = 0$:

$$F(t,\boldsymbol{x}) = \delta(z) f(\boldsymbol{x}) e^{-i\omega t} \text{ with } \boldsymbol{x} = (\boldsymbol{x}, z), \tag{2}$$

and the speed of propagation is spatially heterogeneous

$$\frac{1}{c^2(\boldsymbol{x})} = \frac{1}{c_o^2}\Big[1 + \mu(\boldsymbol{x})\Big], \tag{3}$$

where μ is a zero-mean stationary random process with ergodic properties in the z-direction.

The time-harmonic field $\bar{u}$ such that $u(t,\boldsymbol{x}) = \bar{u}(\boldsymbol{x}) e^{-i\omega t}$ is solution of the random Helmholtz equation

$$(\partial_z^2 + \Delta_\perp)\bar{u} + \frac{\omega^2}{c_o^2}\Big[1 + \mu(\boldsymbol{x}, z)\Big]\bar{u} = -\delta(z) f(\boldsymbol{x}),$$

*Centre de Mathématiques Appliquées, Ecole Polytechnique, 91128 Palaiseau Cedex, France josselin.garnier@polytechnique.edu

where $\Delta_{\vec{x}} = \Delta_\perp + \partial_z^2$. The function $\tilde{\phi}$ (slowly-varying envelope of a plane wave going along the z-axis) defined by

$$\tilde{u}(\boldsymbol{x}, z) = \frac{ic_o}{2\omega} e^{i\omega z/c_o} \tilde{\phi}(\boldsymbol{x}, z) \tag{4}$$

satisfies

$$\partial_z^2 \tilde{\phi} + 2i\frac{\omega}{c_o}\partial_z \tilde{\phi} + \Delta_\perp \tilde{\phi} + \frac{\omega^2}{c_o^2}\mu(\boldsymbol{x}, z)\tilde{\phi} = 2i\frac{\omega}{c_o}\delta(z) f(\boldsymbol{x}). \tag{5}$$

In the paraxial regime "$\lambda \ll l_c, r_o \ll L$" (which means, the wavelength $\lambda = 2\pi c_o/\omega$ is much smaller than the correlation radius l_c of the medium and the radius r_o of the source, which are themselves much smaller than the typical propagation distance L) the forward-scattering approximation in direction z is valid and $\tilde{\phi}$ satisfies the Itô-Schrödinger equation [9]

$$d_z \tilde{\phi} = \frac{ic_o}{2\omega}\Delta_\perp \tilde{\phi} dz + \frac{i\omega}{2c_o}\tilde{\phi} \circ dB(\boldsymbol{x}, z), \qquad \tilde{\phi}(z=0, \boldsymbol{x}) = f(\boldsymbol{x}), \tag{6}$$

where $\circ$ stands for the Stratonovich integral, $B(\boldsymbol{x}, z)$ is a Brownian field, that is a Gaussian process with mean zero and covariance

$$\mathbb{E}[B(\boldsymbol{x}, z)B(\boldsymbol{x}', z')] = \gamma(\boldsymbol{x} - \boldsymbol{x}')\,\min(z, z')$$

with

$$\gamma(\boldsymbol{x}) = \int_{-\infty}^{\infty} \mathbb{E}[\mu(0, 0)\mu(\boldsymbol{x}, z)]dz. \tag{7}$$

Remark: Existence, uniqueness and continuity of solutions to the Itô-Schrödinger model (6) are established in [5]. The proof of the convergence of the solution to (5) to the solution to (6) is in [9]. More precisely, the paraxial regime "$\lambda \ll l_c, r_o \ll L$" corresponds to the scaled regime

$$\omega \to \frac{\omega}{\varepsilon^4}, \qquad \mu(\boldsymbol{x}, z) \to \varepsilon^3 \mu(\boldsymbol{x}/\varepsilon^2, z/\varepsilon^2), \qquad f(\boldsymbol{x}) \to f(\boldsymbol{x}/\varepsilon^2),$$

and the convergence in distribution of the solution to the scaled version of (5) to the solution of the Itô-Schrödinger equation (6) is obtained in the limit $\varepsilon \to 0$.

2 Statistics of the wave field

In this section we describe how to compute the second- and fourth-order moments of the wave field. By Itô's formula and (6), the coherent (or mean) wave satisfies the Schrödinger equation with homogeneous damping:

$$\frac{\partial}{\partial z}\mathbb{E}[\tilde{\phi}] = \frac{ic_o}{2\omega}\Delta_\perp \mathbb{E}[\tilde{\phi}] - \frac{\omega^2 \gamma(0)}{8c_o^2}\mathbb{E}[\tilde{\phi}], \tag{8}$$

and therefore $\mathbb{E}[\tilde{\phi}(\boldsymbol{x}, z)] = \tilde{\phi}_0(\boldsymbol{x}, z)\exp(-z/Z_{\rm sca})$, where $\tilde{\phi}_0$ is the solution in the homogeneous medium and $Z_{\rm sca} = 8c_o^2/[\gamma(0)\omega^2]$. The coherent wave amplitude

decays exponentially with the propagation distance and the characteristic decay length is the *scattering mean free path* $Z_{\rm sca}$. This result shows that any coherent imaging or communication method fails in random media when the propagation distance is larger than the scattering mean free path [8].

The mean Wigner transform defined by

$$W_{\rm m}(\boldsymbol{x},\boldsymbol{\xi},z)=\int_{\mathbb{R}^2}\exp\left(-i\boldsymbol{\xi}\cdot\boldsymbol{y}\right)\mathbb{E}\left\{\phi\left(\boldsymbol{x}+\frac{\boldsymbol{y}}{2},z\right)\overline{\phi}\left(\boldsymbol{x}-\frac{\boldsymbol{y}}{2},z\right)\right\}d\boldsymbol{y} \tag{9}$$

is the angularly-resolved mean wave energy density. By Itô's formula and (6), it solves the *radiative transport equation*

$$\frac{\partial W_{\rm m}}{\partial z}+\frac{c_o}{\omega}\,\boldsymbol{\xi}\cdot\nabla_{\boldsymbol{x}}W_{\rm m}=\frac{\omega^2}{4(2\pi)^2c_o^2}\int_{\mathbb{R}^2}\widehat{\gamma}(\boldsymbol{\kappa})\left[W_{\rm m}(\boldsymbol{\xi}-\boldsymbol{\kappa})-W_{\rm m}(\boldsymbol{\xi})\right]d\boldsymbol{\kappa}, \tag{10}$$

starting from $W_{\rm m}(\boldsymbol{x},\boldsymbol{\xi},z=0)=W_0(\boldsymbol{x},\boldsymbol{\xi})$, the Wigner transform of the initial field f. $\widehat{\gamma}$ is the Fourier transform of γ and determines the scattering cross section of the radiative transport equation. This result shows that the fields observed at nearby points are correlated and their correlations contain information about the medium. Accordingly, one should use local cross correlations for imaging and communication in random media [2, 3].

In order to quantify the stability of correlation-based imaging methods, one needs to evaluate variances of empirical correlations, which involves the fourth-order moment:

$$\begin{aligned}M_4(\boldsymbol{r}_1,\boldsymbol{r}_2,\boldsymbol{q}_1,\boldsymbol{q}_2,z)=\mathbb{E}\Big\{&\phi\left(\frac{\boldsymbol{r}_1+\boldsymbol{r}_2+\boldsymbol{q}_1+\boldsymbol{q}_2}{2},z\right)\overline{\phi}\left(\frac{\boldsymbol{r}_1-\boldsymbol{r}_2+\boldsymbol{q}_1-\boldsymbol{q}_2}{2},z\right)\\&\times\overline{\phi}\left(\frac{\boldsymbol{r}_1+\boldsymbol{r}_2-\boldsymbol{q}_1-\boldsymbol{q}_2}{2},z\right)\overline{\phi}\left(\frac{\boldsymbol{r}_1-\boldsymbol{r}_2-\boldsymbol{q}_1+\boldsymbol{q}_2}{2},z\right)\Big\}.\end{aligned} \tag{11}$$

By Itô's formula and (6), it satisfies the Schrödinger-type equation

$$\frac{\partial M_4}{\partial z}=\frac{ic_o}{\omega}\left(\nabla_{\boldsymbol{r}_1}\cdot\nabla_{\boldsymbol{q}_1}+\nabla_{\boldsymbol{r}_2}\cdot\nabla_{\boldsymbol{q}_2}\right)M_4+\frac{\omega^2}{4c_o^2}\,U_4(\boldsymbol{q}_1,\boldsymbol{q}_2,\boldsymbol{r}_1,\boldsymbol{r}_2)M_4, \tag{12}$$

with the generalized potential

$$\begin{aligned}U_4(\boldsymbol{q}_1,\boldsymbol{q}_2,\boldsymbol{r}_1,\boldsymbol{r}_2)=&\,\gamma(\boldsymbol{q}_2+\boldsymbol{q}_1)+\gamma(\boldsymbol{q}_2-\boldsymbol{q}_1)+\gamma(\boldsymbol{r}_2+\boldsymbol{q}_1)+\gamma(\boldsymbol{r}_2-\boldsymbol{q}_1)\\&-\gamma(\boldsymbol{q}_2+\boldsymbol{r}_2)-\gamma(\boldsymbol{q}_2-\boldsymbol{r}_2)-2\gamma(0).\end{aligned} \tag{13}$$

These moment equations have been known for a long time [13]. If we take the Fourier transform:

$$\begin{aligned}\widehat{M}_4(\boldsymbol{\xi}_1,\boldsymbol{\xi}_2,\boldsymbol{\zeta}_1,\boldsymbol{\zeta}_2,z)=&\int_{\mathbb{R}^8}M_4(\boldsymbol{q}_1,\boldsymbol{q}_2,\boldsymbol{r}_1,\boldsymbol{r}_2,z)\\&\times\exp\left(-i\boldsymbol{q}_1\cdot\boldsymbol{\xi}_1-i\boldsymbol{r}_1\cdot\boldsymbol{\zeta}_1-i\boldsymbol{q}_2\cdot\boldsymbol{\xi}_2-i\boldsymbol{r}_2\cdot\boldsymbol{\zeta}_2\right)d\boldsymbol{r}_1d\boldsymbol{r}_2d\boldsymbol{q}_1d\boldsymbol{q}_2,\end{aligned}$$

then it is possible to prove [11] that in the regime "$\lambda\ll l_c\ll r_o\ll L$" the function $\widehat{M}_4$ has the form

$$\widehat{M}_4(\boldsymbol{\xi}_1,\boldsymbol{\xi}_2,\boldsymbol{\zeta}_1,\boldsymbol{\zeta}_2,z)=\Phi(K,A,f)(\boldsymbol{\xi}_1,\boldsymbol{\xi}_2,\boldsymbol{\zeta}_1,\boldsymbol{\zeta}_2,z), \tag{14}$$

where the nonlinear function Φ is explicit [11, Proposition 1] with

$$K(z) = (2\pi)^8 \exp\left(-\frac{\omega^2}{2c_o^2}\gamma(0)z\right), \tag{15}$$

$$A(\xi,\zeta,z) = \frac{1}{2(2\pi)^2}\int_{\mathbb{R}^2}\exp\left(\frac{\omega^2}{4c_o^2}\int_0^z \gamma\left(x+\frac{c_o\zeta}{\omega}z'\right)dz'\right) - 1\exp\left(-i\xi\cdot x\right)dx, \tag{16}$$

and the approximation holds true in $\mathcal{C}([0,Z], L^1(\mathbb{R}^2\times\mathbb{R}^2\times\mathbb{R}^2\times\mathbb{R}^2))$. These results can now be used to discuss a wide range of applications in imaging and communication.

3 The scintillation index

In this section we study the intensity fluctuations and characterize the scintillation index of the wave field, which quantifies the relative intensity fluctuations. It is a fundamental physical quantity associated for instance with light propagation through the atmosphere [13]. The intensity correlation function is usually defined by [13, Eq. (20.125)]:

$$\Gamma^{(4)}(x,y,z) = \mathbb{E}\left[\left|\phi\left(x+\frac{y}{2},z\right)\right|^2\left|\phi\left(x-\frac{y}{2},z\right)\right|^2\right]. \tag{17}$$

When the initial beam has a Gaussian profile

$$f(x) = \exp\left(-\frac{|x|^2}{r_o^2}\right), \tag{18}$$

we obtain from (14) in the regime "$\lambda \ll l_c \ll r_o \ll L$" that:

$$\begin{aligned}\Gamma^{(4)}(x,y,z) = &-\exp\left(-\frac{\omega^2\gamma(0)z}{2c_o^2}\right)\exp\left(-\frac{2|x|^2}{r_o^2}\right)\\ &+\left(\frac{r_o^2}{4\pi}\right)^2\exp\left(\frac{\omega^2}{4c_o^2}\int_0^z\gamma\left(\zeta\frac{c_oz'}{\omega}\right) - \gamma(0)dz' - \frac{r_o^2|\zeta|^2}{4} + i\zeta\cdot x\right)d\zeta\Big|^2\\ &+\left(\frac{r_o^2}{4\pi}\right)^2\exp\left(\frac{\omega^2}{4c_o^2}\int_0^z\gamma\left(\zeta\frac{c_oz'}{\omega}-y\right) - \gamma(0)dz' - \frac{r_o^2|\zeta|^2}{4} + i\zeta\cdot x\right)d\zeta\Big|^2.\end{aligned} \tag{19}$$

For comparison, the mutual coherence function defined by

$$\Gamma^{(2)}(x,y,z) = \mathbb{E}\left[\phi\left(x+\frac{y}{2},z\right)\overline{\phi}\left(x-\frac{y}{2},z\right)\right] \tag{20}$$

can be obtained by solving (10) and it is given by, in the same regime:

$$\Gamma^{(2)}(x,y,z) = \left(\frac{r_o^2}{4\pi}\right)^2\exp\left(\frac{\omega^2}{4c_o^2}\int_0^z\gamma\left(\zeta\frac{c_oz'}{\omega}-y\right) - \gamma(0)dz' - \frac{r_o^2|\zeta|^2}{4} + i\zeta\cdot x\right)d\zeta. \tag{21}$$

Before giving the result about the scintillation index, we first address the case of a plane wave, which corresponds to the limit case $r_o \to \infty$ and which is addressed in [10] by taking first the limit $r_o \to +\infty$ and then $\lambda \ll l_c \ll L$, and in [11] by taking first the limit $\lambda \ll l_c \ll r_o \ll L$ and then $r_o \to \infty$. It turns out that the two results are identical, which shows that the limits are exchangeable:

$$\lim_{r_o \to \infty} \Gamma^{(2)}(\boldsymbol{x}, \boldsymbol{y}, z) = \exp\left[\frac{\omega^2(\gamma(\boldsymbol{y}) - \gamma(0))z}{4c_o^2}\right],$$

moreover, by (19)

$$\lim_{r_o \to \infty} \Gamma^{(4)}(\boldsymbol{x}, \boldsymbol{y}, z) = 1 - \exp\left[-\frac{\omega^2\gamma(0)z}{2c_o^2}\right] + \exp\left[\frac{\omega^2(\gamma(\boldsymbol{y}) - \gamma(0))z}{2c_o^2}\right].$$

As discussed in [10], this result shows in particular that the scintillation index, that is, the variance of the intensity divided by the square of the mean intensity as defined below in (22), is close to one when $z \gg Z_{\mathrm{sca}}$.

We next consider the scintillation index in the case of an initial Gaussian beam (18) with radius r_o. The scintillation index is usually defined as the square coefficient of variation of the intensity [13, Eq. (20.151)]:

$$S(\boldsymbol{x}, z) = \frac{\mathbb{E}\left[|\phi(\boldsymbol{x}, z)|^4\right] - \mathbb{E}\left[|\phi(\boldsymbol{x}, z)|^2\right]^2}{\mathbb{E}\left[|\phi(\boldsymbol{x}, z)|^2\right]^2}. \tag{22}$$

By the expressions (19) and (21) we can describe the scintillation index of the transmitted beam as follows [11].

Proposition 3.1. *In the regime "$\lambda \ll l_c \ll r_o \ll L$" the scintillation index (22) has the following expression:*

$$S(\boldsymbol{x}, z) = 1 - \frac{\exp\left[-2|\boldsymbol{x}|^2/r_o^2\right]}{\left|\frac{1}{4\pi}\int \exp\left[\frac{\omega^2}{4c_o^2}\int_0^z \gamma\left(\boldsymbol{v}\frac{c_o z'}{\omega r_o}\right)dz' - \frac{|\boldsymbol{v}|^2}{4} + i\boldsymbol{v}\cdot\frac{\boldsymbol{x}}{r_o}\right]d\boldsymbol{v}\right|^2}. \tag{23}$$

Let us consider the following form of the covariance function of the medium fluctuations:

$$\gamma(\boldsymbol{x}) = \gamma(0)\tilde{\gamma}\left[\frac{|\boldsymbol{x}|}{\ell_c}\right],$$

with $\tilde{\gamma}(0) = 1$ and the width of the function $x \to \tilde{\gamma}(x)$ is of order one. For instance, we may consider $\tilde{\gamma}(x) = \exp(-x^2)$. Then the scintillation index at the beam center $\boldsymbol{x} = 0$ is

$$S(z, 0) = 1 - \frac{4}{\left|\int_0^\infty \exp\left[\frac{2z}{Z_{\mathrm{sca}}}\int_0^1 \tilde{\gamma}\left(v\frac{z}{Z_c}s\right)ds - \frac{v^2}{4}\right]vdv\right|^2}, \tag{24}$$

which is a function of z/Z_{sca} and z/Z_c only (or, equivalently, a function of z/Z_{sca} and Z_c/Z_{sca} only), where $Z_c = \omega r_{o\ c}/c_o$ is the typical propagation distance for

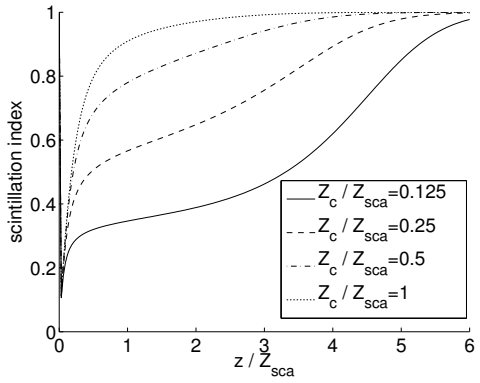

Figure 1: Scintillation index at the beam center (24) as a function of the propagation distance for different values of $Z_{\rm sca}$ and $Z_{\rm c}$. Here $\tilde\gamma(x) = \exp(-x^2)$.

which diffractive effects are of order one, as shown in [9, Eq. (4.4)]. The function (24) is plotted in Figure 1 in the case of Gaussian correlations for the medium fluctuations. It is interesting to note that, even if the propagation distance is larger than the scattering mean free path, the scintillation index can be smaller than one if $Z_{\rm c}$ is small compared to $Z_{\rm sca}$.

In order to get more explicit expressions that facilitate interpretation of the results let us assume that $\gamma(\boldsymbol{x})$ is smooth and can be expanded as

$$\gamma(\boldsymbol{x}) = \gamma(0)\left(1 - \frac{|\boldsymbol{x}|^2}{\ell_{\rm c}^2} + o\left(\frac{|\boldsymbol{x}|^2}{\ell_{\rm c}^2}\right)\right), \qquad \boldsymbol{x} \to 0. \tag{25}$$

When scattering is strong in the sense that the propagation distance is larger than the scattering mean free path $z \gg Z_{\rm sca}$, Eqs. (19) and (21) can be simplified:

$$\Gamma^{(2)}(\boldsymbol{x},\boldsymbol{y},z) = \frac{r_o^2}{r_o^2 + \frac{\gamma(\boldsymbol{0})z^3}{3\ell_{\rm c}^2}} \times \exp\left(-\frac{|\boldsymbol{x}|^2}{r_o^2 + \frac{\gamma(\boldsymbol{0})z^3}{3\ell_{\rm c}^2}} - \frac{\omega^2\gamma(0)z|\boldsymbol{y}|^2}{4c_o^2\ell_{\rm c}^2}\frac{r_o^2 + \frac{\gamma(\boldsymbol{0})z^3}{12\ell_{\rm c}^2}}{r_o^2 + \frac{\gamma(\boldsymbol{0})z^3}{3\ell_{\rm c}^2}} + i\frac{\omega\gamma(0)z^2\boldsymbol{x}\cdot\boldsymbol{y}}{2c_o\ell_{\rm c}^2(r_o^2 + \frac{\gamma(\boldsymbol{0})z^3}{3\ell_{\rm c}^2})}\right), \tag{26}$$

$$\Gamma^{(4)}(\boldsymbol{x},\boldsymbol{y},z) = \left(\frac{r_o^4}{r_o^2 + \frac{\gamma(\boldsymbol{0})z^3}{3\ell_{\rm c}^2}}\right)^2 \times \exp\left(-\frac{2|\boldsymbol{x}|^2}{r_o^2 + \frac{\gamma(\boldsymbol{0})z^3}{3\ell_{\rm c}^2}}\right)\left(1 + \exp\left(-\frac{\omega^2\gamma(0)z|\boldsymbol{y}|^2}{2c_o^2\ell_{\rm c}^2}\frac{r_o^2 + \frac{\gamma(\boldsymbol{0})z^3}{12\ell_{\rm c}^2}}{r_o^2 + \frac{\gamma(\boldsymbol{0})z^3}{3\ell_{\rm c}^2}}\right)\right). \tag{27}$$

This shows that, when $z \gg Z_{\rm sca}$:

- The beam radius is R_z with

$$R_z^2 = r_o^2 + \frac{\gamma(0) z^3}{3\ell_c^2}. \tag{28}$$

- The correlation radius of the intensity distribution is ρ_z with

$$\rho_z^2 = \frac{2c_o^2 \ell_c^2}{2\omega^2 \gamma(0) z} \frac{r_o^2 + \frac{\gamma(0) z^3}{3\ell_c^2}}{r_o^2 + \frac{\gamma(0) z^3}{12\ell_c^2}}, \tag{29}$$

which is of the same order as the correlation radius of the field (compare the $\boldsymbol{y}$-dependence of (26) and (27)).
- The scintillation index is equal to one:

$$S(\boldsymbol{x}, z) = \frac{\Gamma^{(4)}(\boldsymbol{x}, 0, z) - \Gamma^{(2)}(\boldsymbol{x}, 0, z)^2}{\Gamma^{(2)}(\boldsymbol{x}, 0, z)^2} = 1. \tag{30}$$

This observation is consistent with the physical intuition that, in the strongly scattering regime $z/Z_{\rm sca} \gg 1$, the wave field is conjectured to have zero-mean complex circularly symmetric Gaussian statistics, and therefore the intensity is expected to have exponential (or Rayleigh) distribution [6, 13], in agreement with (30).

4 Stability of the Wigner transform

In this section we give an explicit characterization of the signal-to-noise ratio of the Wigner transform. The Wigner transform is a fundamental quadratic form of the field that is useful in the context of analysis of problems involving paraxial or Schrödinger-type equations, for instance time-reversal problems. The Wigner transform of the wave field is defined by

$$W(\boldsymbol{x}, \boldsymbol{\xi}, z) = \int \exp\left[-i\boldsymbol{\xi}\cdot\boldsymbol{y}\right] \phi\left(\boldsymbol{x} + \frac{\boldsymbol{y}}{2}, z\right) \overline{\phi}\left(\boldsymbol{x} - \frac{\boldsymbol{y}}{2}, z\right) d\boldsymbol{y}. \tag{31}$$

It can be interpreted as the angularly-resolved wave energy density (note, however, that it is real-valued but not always non-negative valued). The $\boldsymbol{\xi}$-dependence of the Wigner transform depends on the angular diversity of the initial beam but also on the scattering by the random medium, which dramatically broadens it because the correlation length of the medium is smaller than the initial beam width in our regime of interest "$\lambda \ll l_c \ll r_o \ll L$". As a result the expectation of the Wigner transform is:

$$\begin{aligned}\mathbb{E}[W(\boldsymbol{x}, \boldsymbol{\xi}, z)] = &\frac{r_o^2}{4\pi} \int\int \exp\left[-\frac{r_o^2|\zeta|^2}{4} + i\zeta\cdot\boldsymbol{x} - i\boldsymbol{\xi}\cdot\boldsymbol{y} + \zeta\frac{c_o z}{\omega}\right] \\ &\times \exp\left[\frac{\omega^2}{4c_o^2}\int_0^z \gamma\left(\boldsymbol{y} + \zeta\frac{c_o z'}{\omega}\right) - \gamma(0)\right] dz' \, d\zeta d\boldsymbol{y},\end{aligned} \tag{32}$$

which is the solution of (10). More precisely, the mean Wigner transform can be split into two pieces: a narrow cone and a broad cone in $\boldsymbol{\xi}$:

$$\mathbb{E}[W(\boldsymbol{x},\boldsymbol{\xi},z)] = \frac{K(z)^{1/2}}{(2\pi)^2}\delta(\boldsymbol{\xi})\exp\left(-\frac{|\boldsymbol{x}|^2}{r_o^2}\right) + \frac{r_o^2 K(z)^{1/2}}{(2\pi)^3}\int\exp\left(-\frac{r_o^2|\boldsymbol{\zeta}|^2}{4}+i\boldsymbol{\zeta}\cdot\left(\boldsymbol{x}-\boldsymbol{\xi}\frac{c_o z}{\omega}\right)\right)A(\boldsymbol{\xi},\boldsymbol{\zeta},z)d\boldsymbol{\zeta}. \quad (33)$$

The narrow cone is the contribution of the coherent transmitted wave components and it decays exponentially with the propagation distance (see the expression (15) for $K(z)$). The broad cone is the contribution of the incoherent scattered waves and it becomes dominant when the propagation distance becomes large $z \gg Z_{\rm sca}$.

It is known that the Wigner transform is not statistically stable, and that it is necessary to smooth it (that is to say, to convolve it with a kernel) to get a quantity that can be measured in a statistically stable way (that is to say, the smoothed Wigner transform for one typical realization is approximately equal to its expected value) [1, 17]. Our goal in this section is to quantify this statistical stability.

Let us consider two positive parameters $r_{\rm s}$ and $\xi_{\rm s}$ and define the smoothed Wigner transform:

$$W_{\rm s}(\boldsymbol{x},\boldsymbol{\xi},z) = \frac{1}{(2\pi)^2 r_{\rm s}^2\xi_{\rm s}^2}\int W(\boldsymbol{x}-\boldsymbol{x}',\boldsymbol{\xi}-\boldsymbol{\xi}',z)\exp\left(-\frac{|\boldsymbol{x}'|^2}{2r_{\rm s}^2}-\frac{|\boldsymbol{\xi}'|^2}{2\xi_{\rm s}^2}\right)d\boldsymbol{x}'d\boldsymbol{\xi}'. \quad (34)$$

The expectation of the smoothed Wigner transform is:

$$\mathbb{E}\left[W_{\rm s}(\boldsymbol{x},\boldsymbol{\xi},z)\right] = \frac{r_o^2}{4\pi}\int\exp\left(-\frac{r_o^2|\boldsymbol{\zeta}|^2}{4}-\frac{\xi_{\rm s}^2|\boldsymbol{y}+\boldsymbol{\zeta}\frac{c_o z}{\omega}|^2}{2}-i\boldsymbol{\xi}\cdot\left(\boldsymbol{y}+\boldsymbol{\zeta}\frac{c_o z}{\omega}\right)\right) \times\exp\left(i\boldsymbol{\zeta}\cdot\boldsymbol{x}+\frac{\omega^2}{4c_o^2}\int_0^z\gamma\left(\boldsymbol{y}+\boldsymbol{\zeta}\frac{c_o z'}{\omega}\right)-\gamma(0)dz'\right)d\boldsymbol{\zeta}d\boldsymbol{y}. \quad (35)$$

It can also be written as follows [11].

Proposition 4.1. *The expectation of the smoothed Wigner transform (34) is, in the regime "$\lambda \ll l_c \ll r_o \ll L$":*

$$\mathbb{E}\left[W_{\rm s}(\boldsymbol{x},\boldsymbol{\xi},z)\right] = \frac{K(z)^{1/2}}{(2\pi)^3\xi_{\rm s}^2}\exp\left(-\frac{|\boldsymbol{\xi}|^2}{2\xi_{\rm s}^2}\right)\exp\left(-\frac{|\boldsymbol{x}|^2}{r_o^2}\right) + \frac{K(z)^{1/2}r_o^2}{(2\pi)^4\xi_{\rm s}^2}\int A(\boldsymbol{\xi}',\boldsymbol{\zeta},z)\exp\left(-\frac{r_o^2|\boldsymbol{\zeta}|^2}{4}-\frac{|\boldsymbol{\xi}'-\boldsymbol{\xi}|^2}{2\xi_{\rm s}^2}+i\boldsymbol{\zeta}\cdot\left(\boldsymbol{x}-\boldsymbol{\xi}'\frac{c_o z}{\omega}\right)\right)d\boldsymbol{\zeta}d\boldsymbol{\xi}', \quad (36)$$

where K and A are defined by (15) and (16).

The first term in (36) is a narrow cone in $\boldsymbol{\xi}$ around $\boldsymbol{\xi}=\boldsymbol{0}$ corresponding to coherent wave components and the second term is a broad cone in $\boldsymbol{\xi}$ corresponding to incoherent wave components. Note that the expectation of the smoothed

Wigner transform is independent on r_s as the smoothing in $\boldsymbol{x}$ vanishes in the regime "$\lambda \ll l_c \ll r_o \ll L$". However the smoothing in $\boldsymbol{x}$ plays an important role in the control of the fluctuations of the Wigner transform. We can analyze the variance of the smoothed Wigner transform and its dependence on the smoothing parameters r_s and ξ_s [11].

Proposition 4.2. *The second moment of the smoothed Wigner transform (34) is, in the regime "$\lambda \ll l_c \ll r_o \ll L$":*

$$\begin{aligned}
\mathbb{E}\left[W_s(\boldsymbol{x},\boldsymbol{\xi},z)^2\right] &= \frac{K(z)}{(2\pi)^6\xi_s^4}\exp\left[-\frac{|\boldsymbol{\xi}|^2}{\xi_s^2}\right]\exp\left[-\frac{2|\boldsymbol{x}|^2}{r_o^2}\right]\\
&+\frac{r_o^4K(z)}{(2\pi)^8\xi_s^4}\int\int d\boldsymbol{\xi}_1 d\boldsymbol{\zeta}_1 e^{i\boldsymbol{\zeta}_1\cdot(2\boldsymbol{x}-\frac{c_o z}{\omega}\boldsymbol{\xi}_1)-\frac{r_o^2|\boldsymbol{\zeta}_1|^2}{2}-\frac{|\boldsymbol{\xi}_1-2\boldsymbol{\xi}|^2}{4\xi_s^2}}\\
&\times\Big[4e^{-\frac{|\boldsymbol{\xi}_1|^2}{4\xi_s^2}}\int e^{-i\frac{c_o z}{\omega}\boldsymbol{\xi}_1\cdot\boldsymbol{\zeta}_2-\frac{r_o^2|\boldsymbol{\zeta}_2|^2}{2}}A(\boldsymbol{\xi}_1,\boldsymbol{\zeta}_2+\boldsymbol{\zeta}_1,z)d\boldsymbol{\zeta}_2\\
&+\int\int e^{-\frac{|\boldsymbol{\xi}_2|^2}{4\xi_s^2}-i\frac{c_o z}{\omega}\boldsymbol{\xi}_2\cdot\boldsymbol{\zeta}_2-\frac{r_o^2|\boldsymbol{\zeta}_2|^2}{2}}A\Big(\frac{\boldsymbol{\xi}_2+\boldsymbol{\xi}_1}{2},\boldsymbol{\zeta}_2+\boldsymbol{\zeta}_1,z\Big)\\
&\qquad\times A\Big(\frac{\boldsymbol{\xi}_2-\boldsymbol{\xi}_1}{2},\boldsymbol{\zeta}_2-\boldsymbol{\zeta}_1,z\Big)d\boldsymbol{\xi}_2 d\boldsymbol{\zeta}_2\\
&+4e^{-r_s^2|\boldsymbol{\xi}_1|^2}\int e^{-i\frac{c_o z}{\omega}\boldsymbol{\xi}_1\cdot\boldsymbol{\xi}_2-\frac{r_o^2|\boldsymbol{\xi}_2|^2}{2}}A(\boldsymbol{\xi}_1,\boldsymbol{\xi}_2+\boldsymbol{\zeta}_1,z)d\boldsymbol{\xi}_2\\
&+\int\int e^{-r_s^2|\boldsymbol{\zeta}_2|^2-i\frac{c_o z}{\omega}\boldsymbol{\xi}_2\cdot\boldsymbol{\zeta}_2-\frac{r_o^2|\boldsymbol{\xi}_2|^2}{2}}A\Big(z,\frac{\boldsymbol{\zeta}_2+\boldsymbol{\xi}_1}{2},\boldsymbol{\xi}_2+\boldsymbol{\zeta}_1\Big)\\
&\qquad\times A\Big(\frac{\boldsymbol{\zeta}_2-\boldsymbol{\xi}_1}{2},\boldsymbol{\xi}_2-\boldsymbol{\zeta}_1,z\Big)d\boldsymbol{\xi}_2 d\boldsymbol{\zeta}_2\Big]\quad. \qquad (37)
\end{aligned}$$

This is an exact expression but, as it involves four-dimensional integrals, it is complicated to interpret it. This expression becomes simple in the strongly scattering regime $z \gg Z_{\rm sca}$, because then $A(\boldsymbol{\xi},\boldsymbol{\zeta},z)$ takes a Gaussian form and all integrals can be evaluated. To get more explicit expressions in the discussion of the results we here again assume that $\gamma(\boldsymbol{x})$ can be expanded as (25). When $z \gg Z_{\rm sca}$, we have

$$\begin{aligned}
\mathbb{E}\left[W_s(\boldsymbol{x},\boldsymbol{\xi},z)\right] =& \frac{4\pi c_o^2}{\omega^2\gamma(\mathbf{0})z}\frac{r_o^2}{(r_o^2+\frac{\gamma(\mathbf{0})z^3}{12\ell_c^2})(1+\frac{2c_o^2\xi_s^2\ell_c^2}{\omega^2\gamma(\mathbf{0})z})+\frac{c_o^2z^2\xi_s^2}{2\omega^2}}\\
&\times\exp\left[-\frac{\left|\boldsymbol{x}-\frac{c_o z\boldsymbol{\xi}}{2\omega(1+\frac{2c_o^2\xi_s^2\ell_c^2}{\omega^2\gamma(\mathbf{0})z})}\right|^2}{r_o^2+\frac{\gamma(\mathbf{0})z^3}{12\ell_c^2}+\frac{\frac{c_o^2z^2\xi_s^2}{2\omega^2}}{1+\frac{2c_o^2\xi_s^2\ell_c^2}{\omega^2\gamma(\mathbf{0})z}}}-\frac{|\boldsymbol{\xi}|^2}{\frac{\omega^2\gamma(\mathbf{0})z}{c_o^2\ell_c^2}+2\xi_s^2}\right] \qquad (38)
\end{aligned}$$

and

$$\mathbb{E}\left[W_s(\boldsymbol{x},\boldsymbol{\xi},z)^2\right] = \mathbb{E}\left[W_s(\boldsymbol{x},\boldsymbol{\xi},z)\right]^2\left[1+\frac{(r_o^2+\frac{\gamma(\mathbf{0})z^3}{12\ell_c^2})(1+\frac{2c_o^2\xi_s^2\ell_c^2}{\omega^2\gamma(\mathbf{0})z})+\frac{c_o^2z^2\xi_s^2}{2\omega^2}}{(r_o^2+\frac{\gamma(\mathbf{0})z^3}{12\ell_c^2})(4r_s^2\xi_s^2+\frac{2c_o^2\xi_s^2\ell_c^2}{\omega^2\gamma(\mathbf{0})z})+\frac{c_o^2z^2\xi_s^2}{2\omega^2}}\right]. \qquad (39)$$

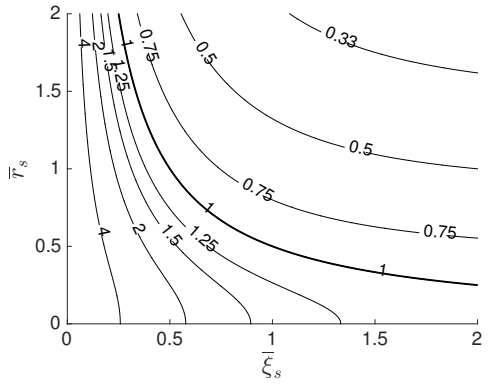

Figure 2: Contour levels of the coefficient of variation (41) of the smoothed Wigner transform. Here $\overline{r}_{\rm s} = r_{\rm s}/\rho_z$ and $\overline{\xi}_{\rm s} = \xi_{\rm s}\rho_z$. The contour level 1 is $2\overline{\xi}_{\rm s}\overline{r}_{\rm s} = 1$.

The coefficient of variation $C_{\rm s}$ of the smoothed Wigner transform, which characterizes its statistical stability, is defined by:

$$C_{\rm s}(\boldsymbol{x},\boldsymbol{\xi},z) = \frac{\sqrt{\mathbb{E}[W_{\rm s}(\boldsymbol{x},\boldsymbol{\xi},z)^2] - \mathbb{E}[W_{\rm s}(\boldsymbol{x},\boldsymbol{\xi},z)]^2}}{\mathbb{E}[W_{\rm s}(\boldsymbol{x},\boldsymbol{\xi},z)]}. \tag{40}$$

We then get the following expression for the coefficient of variation in the strongly scattering regime $z \gg Z_{\rm sca}$ [11].

Proposition 4.3. *Under the same hypotheses as in Propositions 4.1 and 4.2, if additionally $z \gg Z_{\rm sca}$ and γ can be expanded as (25), then the coefficient of variation of the smoothed Wigner transform (34) satisfies:*

$$C_{\rm s}(\boldsymbol{x},\boldsymbol{\xi},z) = \left[\frac{(r_o^2 + \frac{\gamma(\boldsymbol{\theta})z^3}{12\ell_{\rm c}^2})(1 + \frac{2c_o^2\xi_{\rm s}^2\ell_{\rm c}^2}{\omega^2\gamma(\boldsymbol{\theta})z}) + \frac{c_o^2z^2\xi_{\rm s}^2}{2\omega^2}}{(r_o^2 + \frac{\gamma(\boldsymbol{\theta})z^3}{12\ell_{\rm c}^2})(4r_{\rm s}^2\boldsymbol{\xi}_{\rm s}^2 + \frac{2c_o^2\xi_{\rm s}^2\ell_{\rm c}^2}{\omega^2\gamma(\boldsymbol{\theta})z}) + \frac{c_o^2z^2\xi_{\rm s}^2}{2\omega^2}}\right]^{1/2} = \left[\frac{\frac{1}{\xi_{\rm s}^2\rho_z^2} + 1}{\frac{4r_{\rm s}^2}{\rho_z^2} + 1}\right]^{1/2}, \tag{41}$$

where ρ_z is the correlation radius (29).

Note that the coefficient of variation becomes independent of $\boldsymbol{x}$ and $\boldsymbol{\xi}$. Eq. (41) is a simple enough formula to help determining the smoothing parameters $\xi_{\rm s}$ and $r_{\rm s}$ that are needed to reach a given value for the coefficient of variation. The coefficient of variation is plotted in Figure 2, which exhibits the line $2\xi_{\rm s}r_{\rm s} = 1$ separating the two regions where the coefficient of variation is larger or smaller than one:

- For $2\xi_{\rm s}r_{\rm s} = 1$, we have $C_{\rm s}(\boldsymbol{x},\boldsymbol{\xi},z) = 1$.
- For $2\xi_{\rm s}r_{\rm s} < 1$ (resp. > 1) we have $C_{\rm s}(\boldsymbol{x},\boldsymbol{\xi},z) > 1$ (resp. < 1).

- The curve $2\xi_s r_s = 1$ determines the region where the coefficient of variation of $W_s(\boldsymbol{x}, \boldsymbol{\xi}, z)$ is smaller or larger than one (in this regime).

The critical value $r_s = 1/(2\xi_s)$ is indeed special. In this case, the smoothed Wigner transform (34) can be written as the double convolution of the Wigner transform W of the random field $\phi(\cdot, z)$ with the Wigner transform

$$W_g(\boldsymbol{x}, \boldsymbol{\xi}) = \int \exp\left[-i\boldsymbol{\xi}\cdot\boldsymbol{y}\right] \phi_g\left(\boldsymbol{x}+\frac{\boldsymbol{y}}{2}\right)\overline{\phi_g}\left(\boldsymbol{x}-\frac{\boldsymbol{y}}{2}\right) d\boldsymbol{y} \tag{42}$$

of the Gaussian state

$$\phi_g(\boldsymbol{x}) = \exp\left[-\xi_s^2|\boldsymbol{x}|^2\right], \tag{43}$$

since we have

$$W_g(\boldsymbol{x}, \boldsymbol{\xi}) = \frac{2\pi}{\xi_s^2}\exp\left[-2\xi_s^2|\boldsymbol{x}|^2 - \frac{|\boldsymbol{\xi}|^2}{2\xi_s^2}\right],$$

and therefore

$$W_s(\boldsymbol{x}, \boldsymbol{\xi}, z) = \frac{4\xi_s^2}{(2\pi)^3}\int\int W(\boldsymbol{x}-\boldsymbol{x}', \boldsymbol{\xi}-\boldsymbol{\xi}', z) W_g(\boldsymbol{x}', \boldsymbol{\xi}')\, d\boldsymbol{x}'\, d\boldsymbol{\xi}', \tag{44}$$

for $r_s = 1/(2\xi_s)$. It is known that the convolution of a Wigner transform with a kernel that is itself the Wigner transform of a function (such as W_g) is nonnegative real valued (the smoothed Wigner transform obtained with the Gaussian W_g is called Husimi function) [4, 14]. This can be shown easily in our case as the smoothed Wigner transform can be written as

$$W_s(\boldsymbol{x}, \boldsymbol{\xi}, z) = \frac{2\xi_s^2}{\pi}\left|\int \exp\left[i\boldsymbol{\xi}\cdot\boldsymbol{x}'\right]\overline{\phi_g}(\boldsymbol{x}')\phi(\boldsymbol{x}-\boldsymbol{x}', z)\, d\boldsymbol{x}'\right|^2, \tag{45}$$

for $r_s = 1/(2\xi_s)$. From this representation formula of W_s valid for $r_s = 1/(2\xi_s)$, we can see that it is the square modulus of a linear functional of $\phi(\cdot, z)$. The physical intuition that $\phi(\cdot, z)$ has circularly symmetric complex Gaussian statistics in strongly scattering media then predicts that $W_s(\boldsymbol{x}, \boldsymbol{\xi}, z)$ should have an exponential (or Rayleigh) distribution, because the sum of the squares of two independent real-valued Gaussian random variables has an exponential distribution. This is indeed consistent with our theoretical finding that $C_s = 1$ for $r_s = 1/(2\xi_s)$. In fact the situation with complex scattering giving a field that has centered circularly symmetric Gaussian statistics is exactly what motivates the name "scintillation regime" with unit relative intensity fluctuations.

If $r_s > 1/(2\xi_s)$, by observing that

$$\exp\left[-\frac{|\boldsymbol{x}|^2}{2r_s^2}\right] = \Psi(\boldsymbol{x}) *_{\boldsymbol{x}} \exp\left[-2\xi_s^2|\boldsymbol{x}|^2\right],$$

where $*_{\boldsymbol{x}}$ stands for the convolution product in $\boldsymbol{x}$:

$$\Psi(\boldsymbol{x}) *_{\boldsymbol{x}} f(\boldsymbol{x}) = \int \Psi(\boldsymbol{x}-\boldsymbol{x}')f(\boldsymbol{x}')\, d\boldsymbol{x}',$$

and the function Ψ is defined by

$$\Psi(\boldsymbol{x}) = \frac{8\xi_{\rm s}^4 r_{\rm s}^2}{\pi(4\xi_{\rm s}^2 r_{\rm s}^2 - 1)} \exp\left(- \frac{2\xi_{\rm s}^2 |\boldsymbol{x}|^2}{(4\xi_{\rm s}^2 r_{\rm s}^2 - 1)} \right), \tag{46}$$

we observe that the smoothed Wigner transform (34) can be expressed as:

$$W_{\rm s}(z, \boldsymbol{x}, \boldsymbol{\xi}) = \Psi(\boldsymbol{x}) *_{\boldsymbol{x}} \left(\frac{2\xi_{\rm s}^2}{\pi} \right)^2 \exp\left(i\boldsymbol{\xi} \cdot \boldsymbol{x}' \right) \overline{\phi_{\rm g}}(\boldsymbol{x}') \phi(\boldsymbol{x} - \boldsymbol{x}', z) d\boldsymbol{x}' \Big|^2, \tag{47}$$

for $r_{\rm s} > 1/(2\xi_{\rm s})$. From this representation formula for $W_{\rm s}$ valid for $r_{\rm s} > 1/(2\xi_{\rm s})$, we can see that it is nonnegative valued and that it is a local average of (45), which has a unit coefficient of variation in the strongly scattering scintillation regime. That is why the coefficient of variation of the smoothed Wigner transform is smaller than one when $r_{\rm s} > 1/(2\xi_{\rm s})$.

Finally, it is possible to take $r_{\rm s} = 0$ in (34), which corresponds to the absence of smoothing in $\boldsymbol{x}$:

$$W_{\rm s}(\boldsymbol{x}, \boldsymbol{\xi}, z) = \frac{1}{2\pi\xi_{\rm s}^2} \int W(\boldsymbol{x}, \boldsymbol{\xi} - \boldsymbol{\xi}', z) \exp\left(- \frac{|\boldsymbol{\xi}'|^2}{2\xi_{\rm s}^2} \right) d\boldsymbol{\xi}',$$

for $r_{\rm s} = 0$. We then get

$$\begin{aligned}
&\mathrm{Var}\left[W_{\rm s}(\boldsymbol{x}, \boldsymbol{\xi}, z) \right] \\
&= \left(\frac{\frac{4\pi c_o^2 r_o^2 \ell_{\rm c}^2}{\omega^2 \gamma(\boldsymbol{\theta}) z}}{(r_o^2 + \frac{\gamma(\boldsymbol{\theta}) z^3}{12\ell_{\rm c}^2})(1 + \frac{2c_o^2 \xi_{\rm s}^2 \ell_{\rm c}^2}{\omega^2 \gamma(\boldsymbol{\theta}) z}) + \frac{c_o^2 z^2 \xi_{\rm s}^2}{2\omega^2}} \right)^2 \\
&\quad \times \exp\left(- \frac{2\left| \boldsymbol{x} - \frac{c_o z \boldsymbol{\xi}}{2\omega(1 + \frac{2c_o^2 \xi_{\rm s}^2 \ell_{\rm c}^2}{\omega^2 \gamma(\boldsymbol{\theta}) z})} \right|^2}{r_o^2 + \frac{\gamma(\boldsymbol{\theta}) z^3}{12\ell_{\rm c}^2} + \frac{\frac{c_o^2 z^2 \xi_{\rm s}^2}{2\omega^2}}{1 + \frac{2c_o^2 \xi_{\rm s}^2 \ell_{\rm c}^2}{\omega^2 \gamma(\boldsymbol{\theta}) z}}} - \frac{2|\boldsymbol{\xi}|^2}{\frac{\omega^2 \gamma(\boldsymbol{\theta}) z}{c_o^2 \ell_{\rm c}^2} + 2\xi_{\rm s}^2} \right)
\end{aligned}$$

and

$$C_{\rm s}(\boldsymbol{x}, \boldsymbol{\xi}, z) = \sqrt{1 + (\xi_{\rm s} \rho_z)^{-2}},$$

for $r_{\rm s} = 0$. If, additionally, we let $\xi_{\rm s} \to \infty$, then we find

$$\begin{aligned}
&\lim_{\xi_{\rm s} \to \infty} \frac{\xi_{\rm s}^2}{2\pi} \mathbb{E}\left[W_{\rm s}(\boldsymbol{x}, \boldsymbol{\xi}, z) \right] = \frac{r_o^2}{r_o^2 + \frac{\gamma(\boldsymbol{\theta}) z^3}{3\ell_{\rm c}^2}} \exp\left(- \frac{|\boldsymbol{x}|^2}{r_o^2 + \frac{\gamma(\boldsymbol{\theta}) z^3}{3\ell_{\rm c}^2}} \right), \\
&\lim_{\xi_{\rm s} \to \infty} \left(\frac{\xi_{\rm s}^2}{2\pi} \right)^2 \mathrm{Var}\left[W_{\rm s}(\boldsymbol{x}, \boldsymbol{\xi}, z) \right] = \left(\frac{r_o^2}{r_o^2 + \frac{\gamma(\boldsymbol{\theta}) z^3}{3\ell_{\rm c}^2}} \right)^2 \exp\left(- \frac{2|\boldsymbol{x}|^2}{r_o^2 + \frac{\gamma(\boldsymbol{\theta}) z^3}{3\ell_{\rm c}^2}} \right),
\end{aligned}$$

and also

$$\lim_{\xi_{\rm s} \to \infty} C_{\rm s}(\boldsymbol{x}, \boldsymbol{\xi}, z) = 1,$$

for $r_{\rm s} = 0$. These results are consistent with formulas (26-27) (with $\boldsymbol{y} = \boldsymbol{0}$), formula (30), and the fact that

$$\left| \phi(\boldsymbol{x}, z) \right|^2 = \frac{1}{(2\pi)^2} \int W(\boldsymbol{x}, \boldsymbol{\xi}', z) d\boldsymbol{\xi}' = \lim_{\xi_{\rm s} \to \infty} \frac{\xi_{\rm s}^2}{2\pi} W_{\rm s}(\boldsymbol{x}, \boldsymbol{\xi}, z) \mid_{r_{\rm s}=0}.$$

5 Applications to imaging and communication

We finally remark that the results reported here can be useful in the analysis of ghost imaging experiments [19], enhanced focusing [20] and super-resolution imaging problems [15], and intensity correlation-based imaging and communication [16, 18].

Ghost imaging is a fascinating recent imaging methodology. It can be interpreted as a correlation-based imaging technique since it gives an image of an object by correlating the intensities measured by two detectors, a high-resolution detector that does not view the object and a low-resolution detector that does view the object. The resolution of the image depends on the coherence properties of the sources used to illuminate the object, and on the scattering properties of the medium. This problem can be understood at the mathematical level by using the results presented in [7].

Enhanced focusing refers to schemes for communication and imaging in a case where a reference signal propagating through the random medium is available. This information can be used to design an optimal probe that focuses tightly at the desired target point. How to optimally design and analyze such schemes, given the limitations of the transducers and so on, can be analyzed using the moment theory presented in [12]. More generally *super resolution* refers situations where one tries to go beyond the classic diffraction limited resolution in imaging systems.

Intensity correlations is a recently proposed scheme for communication and imaging in the optical regime that is based on using cross corrections of intensities. This is a promising scheme for communication and imaging through relatively strong clutter. By using the correlation of the intensity or speckle for different incoming angles or different positions of the source one can get spatial information about the source. The idea of using the information about the statistical structure of speckle to enhance signaling is very interesting and corroborates the idea that modern schemes for communication and imaging require a mathematical theory for analysis of high-order moments.

The results reported here have already opened the mathematical analysis of important imaging problems and we believe that many more problems than those mentioned here will benefit from the results regarding the fourth moments. In fact, enhanced transducer technology and sampling schemes allow for using finer aspects of the wave field involving second- and fourth-order moments and in such complex cases a rigorous mathematical analysis is important to support, complement, or sometimes disprove, statements based on physical intuition alone.

References

[1] G. Bal, *On the self-averaging of wave energy in random media*, SIAM Multiscale Model. Simul. **2** (2004), 398–420.

[2] L. Borcea, G. Papanicolaou, and C. Tsogka, *Interferometric array imaging in clutter*, Inverse Problems **21** (2005), 1419–1460.

[3] L. Borcea, J. Garnier, G. Papanicolaou, and C. Tsogka, *Enhanced statistical stability in coherent interferometric imaging*, Inverse Problems **27** (2011), 085004.

[4] N. D. Cartwright, *A non-negative Wigner-type distribution*, Physica **83A** (1976), 210–212.

[5] D. Dawson and G. Papanicolaou, *A random wave process*, Appl. Math. Optim. **12** (1984), 97–114.

[6] R. L. Fante, *Electromagnetic beam propagation in turbulent media*, Proc. IEEE **63** (1975), 1669–1692.

[7] J. Garnier, *Ghost imaging in the random paraxial regime*, Inverse Problems and Imaging **10** (2016), 409–432.

[8] J. Garnier and G. Papanicolaou, *Passive Imaging with Ambient Noise*, Cambridge University Press, Cambridge, 2016.

[9] J. Garnier and K. Sølna, *Coupled paraxial wave equations in random media in the white-noise regime*, Ann. Appl. Probab. **19** (2009), 318–346.

[10] J. Garnier and K. Sølna, *Scintillation in the white-noise paraxial regime*, Comm. Part. Differ. Equat. **39** (2014), 626–650.

[11] J. Garnier and K. Sølna, *Fourth-moment analysis for beam propagation in the white-noise paraxial regime*, Archive on Rational Mechanics and Analysis **220** (2016), 37–81.

[12] J. Garnier and K. Sølna, *Focusing waves through a randomly scattering medium in the white-noise paraxial regime*, SIAM J. Appl. Math. **77** (2017), 500–519.

[13] A. Ishimaru, *Wave Propagation and Scattering in Random Media*, Academic Press, San Diego, 1978.

[14] G. Manfredi and M. R. Feix, *Entropy and Wigner functions*, Phys. Rev. E **62** (2000), 4665–4674.

[15] A. P. Mosk, A. Lagendijk, G. Lerosey, and M. Fink, *Controlling waves in space and time for imaging and focusing in complex media*, Nature Photon. **6** (2012), 283–292.

[16] J. A. Newman and K. J. Webb, *Fourier magnitude of the field incident on a random scattering medium from spatial speckle intensity correlations*, Opt. Lett. **37** (2012), 1136–1138.

[17] G. Papanicolaou, L. Ryzhik, and K. Sølna, *Self-averaging from lateral diversity in the Itô-Schrödinger equation*, SIAM Multiscale Model. Simul. **6** (2007), 468–492.

[18] S. Popoff, G. Lerosey, M. Fink, A. C. Boccara, and S. Gigan, *Image transmission through an opaque material*, Nature Commun. **1** (2010), 1–5.

[19] J. H. Shapiro and R. W. Boyd, *The physics of ghost imaging*, Quantum Inf. Process. **11** (2012), 949–993.

[20] I. M. Vellekoop and A. P. Mosk, *Focusing coherent light through opaque strongly scattering media*, Opt. Lett. **32** (2007), 2309–2311.